

# Scalar-Quark Systems and Chimera Hadrons in $SU(3)_c$ Lattice QCD

H. Iida<sup>1\*</sup>, H. Suganuma<sup>2</sup> and T. T. Takahashi<sup>1</sup>

<sup>1</sup> Yukawa Institute for Theoretical Physics, Kyoto University, Sakyo, Kyoto 606-8502, Japan and

<sup>2</sup>Department of Physics, Kyoto University, Kitashirakawaoiwake, Sakyo, Kyoto 606-8502, Japan

(Dated: February 8, 2020)

Light scalar-quarks  $\phi$  (colored scalar particles or idealized diquarks) and their color-singlet hadronic states are studied with quenched  $SU(3)_c$  lattice QCD in terms of mass generation in strong interaction without chiral symmetry breaking. We investigate “scalar-quark mesons”  $\phi^\dagger\phi$  and “scalar-quark baryons”  $\phi\phi\phi$  which are the bound states of scalar-quarks  $\phi$ . We also investigate the bound states of scalar-quarks  $\phi$  and quarks  $\psi$ , i.e.,  $\phi^\dagger\psi$ ,  $\psi\psi\phi$  and  $\phi\phi\psi$ , which we name “chimera hadrons”. All the new-type hadrons including  $\phi$  are found to have a large mass even for zero bare scalar-quark mass  $m_\phi = 0$  at  $a^{-1} \simeq 1\text{GeV}$ . We find that the constituent scalar-quark and quark picture is satisfied for all the new-type hadrons. Namely, the mass of the new-type hadron composed of  $m$   $\phi$ ’s and  $n$   $\psi$ ’s,  $M_{m\phi+n\psi}$ , satisfies  $M_{m\phi+n\psi} \simeq mM_\phi + nM_\psi$ , where  $M_\phi$  and  $M_\psi$  are the constituent scalar-quark and quark mass, respectively.  $M_\phi$  at  $m_\phi = 0$  estimated from these new-type hadrons is  $1.5\text{-}1.6\text{GeV}$ , which is larger than that of light quarks,  $M_\psi \simeq 400\text{MeV}$ . Therefore, in the systems of scalar-quark hadrons and chimera hadrons, scalar-quarks acquire large mass due to large quantum corrections by gluons. Together with other evidences of mass generations of glueballs and charmonia, we conjecture that all colored particles generally acquire a large effective mass due to dressed gluon effects.

PACS numbers: 12.38.Gc, 14.80.-j, 14.80.Ly

## I. INTRODUCTION

The origin of mass is one of the fundamental and fascinating subjects in physics for a long time. A standard interpretation of mass origin is the interaction with the Higgs field [1]. However, the mass of Higgs origin is only about 1% of total mass in the world, because the Higgs interaction only provides the current quark mass (less than  $10\text{MeV}$  for light quarks) and the lepton mass ( $0.51\text{MeV}$  for electrons) [2]. On the other hand, apart from unknown dark matter, about 99% of mass of matter in the world originates from the strong interaction, which actually provides the large constituent quark mass  $M_\psi = (300 - 400)\text{MeV}$  [3]. Such a dynamical fermion-mass generation in the strong interaction can be interpreted as spontaneous breaking of chiral symmetry, which was first pointed out by Y. Nambu et al. [4]. According to the chiral symmetry breaking, light quarks are considered to have a large constituent quark mass of about  $400\text{MeV}$ . In terms of the mass-generation mechanism, it is interesting to investigate high density and/or high temperature systems, because chiral symmetry is expected to be restored in the system [5, 6, 7]. Several theoretical studies suggest that such a restoration affects the hadron nature [6, 7, 8, 9]. Actually, the experiments at CERN SPS [10] and KEK [11] indicate the change of nature of the vector mesons  $\rho$ ,  $\omega$  and  $\phi$  in finite density system. These experiments are important for the study of the mass generation originated from chiral symmetry breaking.

Then, a question arises: Is there any mechanism of dynamical mass generation without chiral symmetry breaking? To answer this question, we note the following examples supporting the existence of such a mechanism. One example is gluons, colored vector particles in QCD. While the gluon is massless in perturbation QCD, non-perturbative effects due to the self-interaction of gluons seem to generate a large effective gluon mass as  $(0.5\text{-}1.0)\text{GeV}$ , which is measured in lattice QCD [12, 13]. Actually, glueballs, which are composed of gluons, have a large mass, e.g., about  $1.5\text{GeV}$  [14] even for the lightest glueball ( $JPC = 0^{++}$ ), and scalar meson  $f_0(1500)$  is one of the candidate of the  $0^{++}$  glueball in experimental side [2]. Another example is charm quarks. The current mass of charm quarks is about  $1.2\text{GeV}$  at the renormalization point  $\mu = 1\text{GeV}$  [2]. In the quark model, however, the constituent charm-quark mass which reproduces masses of charmonia is set about  $1.6\text{GeV}$  [3]. The about  $400\text{MeV}$  difference between the current and the constituent charm-quark masses can be explained as dynamical mass generation without chiral symmetry breaking, since there is no chiral symmetry for such a heavy quark system.

These examples suggest that there is another type of mass generation without chiral symmetry breaking and the Higgs mechanism. Then, we conjecture that, even without chiral symmetry breaking, large dynamical mass generation generally occurs in the strong interaction, i.e., *all colored particles have a large effective mass generated by dressed gluon effects*.

The study is also motivated by diquark picture of hadrons. Diquark is made of two quarks which are strongly correlated in color anti-triplet  $\bar{\mathbf{3}}$  channel. Sometimes, diquarks are treated as point-like objects, i.e., localized bosons. Degrees of freedom of diquarks is im-

\*E-mail: iida@yukawa.kyoto-u.ac.jp

portant in some aspects of hadron physics. For example, nucleon structure function can be explained by the model in which nucleon is the admixture of diquark and quark [15, 16]. Diquark is also important for hadron spectra [17, 18]. In high density system, diquark condensation is considered to appear due to the attractive interaction of one-gluon exchange in color  $\bar{\mathbf{3}}$  channel. Such a phase is called color superconductivity phase [19, 20] and it may exist in the interior of neutron stars. However, the nature of diquarks as a real object, its size and mass for example, is not well understood. It is then desired to clarify the diquark picture in terms of the fundamental and reliable way. Point-like limit of diquark in color  $\bar{\mathbf{3}}$  channel can be regarded as the scalar-quark in fundamental representation of  $SU(3)_c$  in scalar QCD [21]. Therefore, theoretical study of scalar-quarks with reliable method is expected to be a good test place to check the validity of the point-like diquark picture.

According to these motivations, we study the scalar-quark and their color-singlet hadronic states using quenched  $SU(3)_c$  lattice QCD [22]. We investigate the masses of “scalar-quark hadrons” which are the bound states of scalar-quarks  $\phi$  and “chimera hadrons” which are the bound states of  $\phi$  and (ordinary) quarks  $\psi$ . The temporal correlators of these hadrons are calculated in quenched lattice QCD, and their mass of lowest energy state is extracted from the correlators. As a result, we find the large mass of these hadrons including scalar-quarks  $\phi$ . Also we find that the constituent scalar-quark and quark picture is satisfied for all the new-type hadrons. Namely, the mass of the new-type hadron which is composed of  $m$   $\phi$ ’s and  $n$   $\psi$ ’s,  $M_{m\phi+n\psi}$ , satisfies  $M_{m\phi+n\psi} \simeq mM_\phi + nM_\psi$ , where  $M_\phi$  and  $M_\psi$  are the constituent scalar-quark and quark mass, respectively. The  $M_\phi$  estimated from these new hadrons is 1.5–1.6GeV, which is larger than the constituent quark mass  $M_\psi \simeq 400$ MeV for light quarks. These results suggest that in the system of scalar particles, there occurs large mass generation in the strong interaction without chiral symmetry breaking.

The article is organized as follows. In Sec. II, the new states including scalar-quarks, “scalar-quark hadrons” and “chimera hadrons”, are introduced. In Sec. III, calculation method of the mass of the new hadrons are explained. We show the setup of lattice QCD and the method to extract the lowest energy state of these hadrons from temporal correlators. In Sec. IV and V, we show the numerical results of the scalar-quark hadrons and the chimera hadrons. Sec. VI is devoted to conclude and discuss our results.

## II. NEW STATES INCLUDING SCALAR-QUARKS

In this section, we explain the new-type hadrons introduced in the study. We study the mass generation mechanism of scalar-quarks by investigating the color-



FIG. 1: Diagrams for scalar-quark hadrons. The left-hand side figure denotes the two-point correlator of scalar-quark meson ( $\phi^\dagger\phi$ ) and the right-hand side figure denotes that of scalar-quark baryon ( $\phi\phi\phi$ ). The dotted line corresponds to the scalar-quark  $\phi$ . We only evaluate connected diagrams of scalar-quark meson. Disconnected diagram is not included in this study.

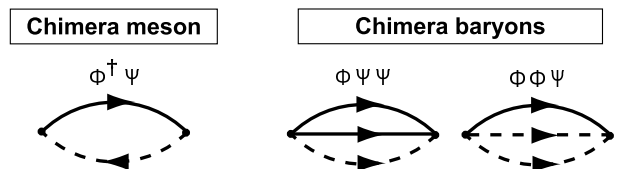


FIG. 2: Diagrams for chimera hadrons. The left-hand side figure denotes the two point correlator of chimera meson ( $\phi^\dagger\psi$ ) and the two figures of right-hand side denote that of chimera baryons ( $\phi\psi\psi$  and  $\phi\phi\psi$ ). The dotted line corresponds to the scalar-quark  $\phi$  and the solid line corresponds to the (ordinary) quark  $\psi$ .

singlet states including scalar-quarks. We call the color-singlet state which is composed only of scalar-quarks  $\phi$  as “scalar-quark hadron”: scalar-quark meson is composed of a scalar-quark and an anti scalar-quark,  $\phi^\dagger\phi$ , and scalar-quark baryon is made of three scalar-quarks,  $\phi\phi\phi$ . We also call the color-singlet state which is made of scalar-quarks  $\phi$  and (ordinary) quarks  $\psi$  “chimera hadron”: chimera meson  $\phi^\dagger\psi$ , chimera baryon  $\phi\phi\psi$  and chimera baryon  $\phi\psi\psi$ . Here, we note that the statistics for these hadrons are different from that of ordinary hadrons. For example, scalar-quark baryon  $\phi\phi\phi$  is a boson and chimera meson  $\phi^\dagger\psi$  is a fermion, although ordinary baryon is a fermion and ordinary meson is a boson.

Figures 1 and 2 show the schematic figures of two-point correlators for scalar-quark hadrons and chimera hadrons, respectively. In this calculation, we assume that fields in a hadronic operator have all different “flavors”. Due to the assumption, disconnected diagram of scalar-quark meson is omitted in the study.

We investigate only  $J^P = 0^+$  state, because the state is the lowest and therefore is suitable for the investigation of the mass generation of scalar-quarks. Table I is the summary of the names of the new hadrons, Lorentz properties and the operators we use.

TABLE I: Summary table of new-type hadrons, i.e., scalar-quark hadrons and chimera hadrons. Names, Lorentz properties and operators used for our lattice calculation are listed.

|                     |                      |        |   |
|---------------------|----------------------|--------|---|
| Scalar-quark meson  | $(\phi^\dagger\phi)$ | Scalar | $M_s(x) \equiv \phi_a^\dagger(x)\phi_a(x)$                              |
| Scalar-quark baryon | $(\phi\phi\phi)$     | Scalar | $B_s(x) \equiv \epsilon_{abc}\phi_a(x)\phi_b(x)\phi_c(x)$               |
| Chimera meson       | $(\phi^\dagger\psi)$ | Spinor | $C_M^\alpha(x) \equiv \phi_a^\dagger(x)\psi_a^\alpha(x)$                |
| Chimera baryon      | $(\psi\psi\phi)$     | Scalar | $C_B(x) \equiv \epsilon_{abc}(\psi_a^T(x)C\gamma_5\psi_b(x))\phi_c(x)$  |
| Chimera baryon      | $(\phi\phi\psi)$     | Spinor | $C_B^\alpha(x) \equiv \epsilon_{abc}\phi_a(x)\phi_b(x)\psi_c^\alpha(x)$ |

### III. FORMALISM AND SETUP OF LATTICE QCD

In this section, formalism and setup of lattice QCD calculation is explained. To include scalar-quarks  $\phi$  together with quarks  $\psi$  and gluons in QCD, we adopt the generalized QCD Lagrangian density in the continuum limit and Minkowski space,

$$\mathcal{L} = -\frac{1}{4}G_{\mu\nu}^a G^{a\mu\nu} + \mathcal{L}_F + \mathcal{L}_{SQ}, \quad (1)$$

$$\mathcal{L}_F = \bar{\psi}(i\mathcal{D} - m_\psi)\psi, \quad (2)$$

$$\mathcal{L}_{SQ} = \text{tr}(D_\mu\phi)^\dagger(D^\mu\phi) - m_\phi^2 \text{tr}\phi^\dagger\phi, \quad (3)$$

where  $m_\psi$  and  $m_\phi$  are bare masses of scalar-quarks and quarks, respectively.  $G_{\mu\nu}^a$  denotes the field strength tensor,

$$G_{\mu\nu}^a \equiv \partial_\mu A_\nu^a - \partial_\nu A_\mu^a + gf^{abc}A_\mu^b A_\nu^c, \quad (4)$$

where  $A_\mu^a$  is gluon field,  $f^{abc}$  is structure function of SU(3) and  $\mathcal{D} \equiv \gamma^\mu D_\mu$  denotes the covariant derivative,

$$D_\mu \equiv \partial_\mu - igA_\mu. \quad (5)$$

In the calculation on lattice, we need discretized Euclidean lattice action. For the gluon sector, we adopt the standard Wilson action [23],

$$S_G \equiv \frac{\beta}{N_c} \sum_{x,\mu,\nu} \text{ReTr}\{1 - P_{\mu\nu}(x)\}, \quad (6)$$

where  $\beta \equiv 2N_c/g^2$  and  $P_{\mu\nu}(x)$  is plaquette,

$$P_{\mu\nu} \equiv U_\mu(x)U_\nu(x + \hat{\mu})U_\mu^\dagger(x + \hat{\nu})U_\nu^\dagger(x), \quad (7)$$

where  $U_\mu(x)$  is link variable.  $\hat{\mu}$  and  $\hat{\nu}$  denote the unit vectors of the direction  $\mu$  and  $\nu$  on lattice, respectively.

For the quark part, we use the Wilson fermion action [23],

$$\begin{aligned} S_F &\equiv \sum_{x,y} \bar{\psi}(x)K(x,y)\psi(y), \\ K(x,y) &\equiv \delta_{x,y} - \kappa \sum_\mu \{(\mathbf{1} - \gamma_\mu)U_\mu(x)\delta_{x+\hat{\mu},y} \\ &\quad + (\mathbf{1} + \gamma_\mu)U_\mu^\dagger(y)\delta_{x,y+\hat{\mu}}\}, \end{aligned} \quad (8)$$

where  $\kappa$  is hopping parameter which is related to the bare quark mass  $m_\psi$ .

For scalar-quarks, we use the following action,

$$S_{SQ} \equiv \sum_{x,y} \phi^\dagger(x) \{- \sum_\mu (\delta_{x+\hat{\mu},y}U_\mu(x) + \delta_{x-\hat{\mu},y}U_\mu^\dagger(y) \\ - 2\delta_{xy}\mathbf{1}) + m_\phi^2\delta_{xy}\mathbf{1}\} \phi(y). \quad (9)$$

This action is local and the simplest one which is gauge invariant.

We set  $\beta \equiv 2N_c/g^2 = 5.70$ , which corresponds to the lattice spacing  $a \simeq 0.18\text{fm} = (1.1\text{GeV})^{-1}$  [24]. We adopt  $16^3 \times 32$  lattice, which corresponds to the spatial volume  $V \simeq (2.9\text{fm})^3$ . The number of the gauge configurations  $N_{\text{conf}}$  is 100. We take the configurations every 500 sweeps after 20000 thermalization. For the bare scalar-quark mass,  $m_\phi = 0.0, 0.11, 0.22$  and  $0.33\text{GeV}$  are adopted. For the bare quark mass, we take the hopping parameters  $\kappa = 0.1650, 0.1625$  and  $0.1600$ . If we assume the relation  $2m_\psi a = 1/\kappa - 1/\kappa_c$ , where  $\kappa_c$  is the hopping parameter in which pion is massless, corresponding bare quark masses  $m_\psi$  are  $0.09, 0.14$  and  $0.19\text{GeV}$  [25]. These parameters are summarized in table II. In table III, the mass of pion, rho meson and nucleon for each  $\kappa$  on our lattice are shown. Bare quark masses  $m_\psi$  at each hopping parameters  $\kappa$  at the lattice cutoff  $a^{-1} \simeq 1.1\text{GeV}$  are also listed in table III.

We calculate the following temporal correlator  $G(t)$  of hadronic operator  $O(x, t)$ ,

$$G(t) \equiv \frac{1}{V} \sum_{\vec{x}} \langle O(\vec{x}, t)O^\dagger(\vec{0}, 0) \rangle, \quad (10)$$

where the total momentum is projected to be zero. To extract the lowest-state mass  $M_0$  of a hadron, we fit the temporal correlator by the single exponential function  $G_{\text{fit}}(t) = A \exp(-M_0 t)$ , in the region where the lowest energy state dominates. For the determination of the fit range, we construct so-called effective mass,

$$m_{\text{eff}}(t) \equiv -\ln \frac{G(t)}{G(t+1)}. \quad (11)$$

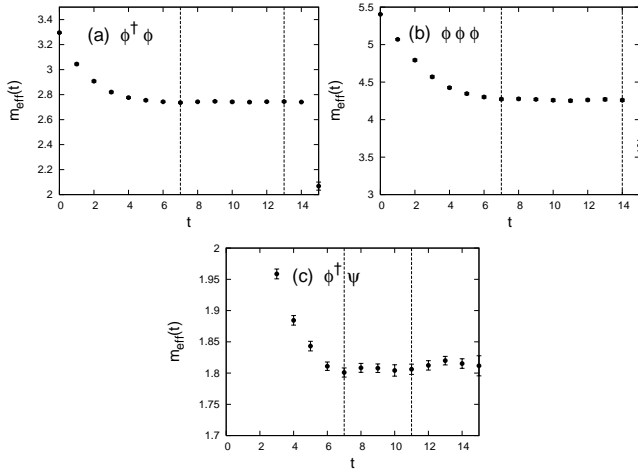
If  $G(t)$  is dominated by lowest state with mass  $M_0$  in a certain region for large  $t$ , then  $m_{\text{eff}}(t) \simeq M_0$  for the  $t$  region. In other words, if there is a plateau region of  $m_{\text{eff}}(t)$  for large  $t$ , the correlator is dominated by the lowest energy state for the  $t$  region. Therefore, we set the fit range of the correlator to the corresponding plateau region of effective mass. Figure 3 is the examples of effective masses for (a) scalar-quark meson  $\phi^\dagger\phi$ , (b) scalar-quark baryon  $\phi\phi\phi$  and (c) chimera meson  $\phi^\dagger\psi$ . In these

TABLE II: Parameters of lattice QCD. The lattice spacing  $a^{-1}$  is set by string tension  $\sigma \simeq 0.89 \text{ GeV/fm}$  [24].

| $\beta$ | Lattice size     | $a^{-1}$ | $N_{\text{conf}}$ | bare scalar-quark mass $m_\phi$ | $\kappa$               |
|---------|------------------|----------|-------------------|---------------------------------|------------------------|
| 5.70    | $16^3 \times 32$ | 1.1 GeV  | 100               | 0.00, 0.11, 0.22, 0.33 GeV      | 0.1650, 0.1625, 0.1600 |

TABLE III: Masses of  $\pi$  (pseudoscalar meson),  $\rho$  (vector meson) and  $N$  (nucleon) for each  $\kappa$ . The unit is GeV.  $\chi^2$  per degrees of freedom  $N_{\text{df}}$  is added. The error estimate is done by the jackknife method. We also add  $m_\psi$  estimated from the relation  $2m_\psi a = 1/\kappa - 1/\kappa_c$ , where the critical hopping parameter  $\kappa_c = 0.1694$  [25].

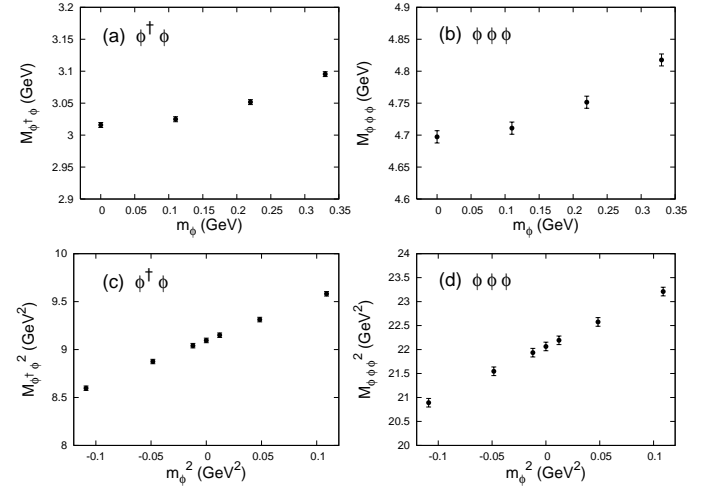
| $\kappa$ | $M_\pi$ ( $\chi^2/N_{\text{df}}$ ) | $M_\rho$ ( $\chi^2/N_{\text{df}}$ ) | $M_N$ ( $\chi^2/N_{\text{df}}$ ) | $m_\psi$ |
|----------|------------------------------------|-------------------------------------|----------------------------------|----------|
| 0.1650   | $0.4926 \pm 0.0036$ (0.748)        | $0.7177 \pm 0.0091$ (2.772)         | $1.1551 \pm 0.0021$ (1.426)      | 0.087    |
| 0.1625   | $0.6303 \pm 0.0035$ (0.599)        | $0.7969 \pm 0.0063$ (1.462)         | $1.2934 \pm 0.0017$ (0.627)      | 0.14     |
| 0.1600   | $0.7510 \pm 0.0036$ (0.715)        | $0.8791 \pm 0.0053$ (0.955)         | $1.4453 \pm 0.0013$ (0.817)      | 0.19     |

FIG. 3: Typical examples of effective mass plots for (a) scalar-quark meson  $\phi^\dagger \psi$  at  $m_\phi = 0$ , (b) scalar-quark baryon  $\phi \phi \phi$  at  $m_\phi = 0$  and (c) chimera meson  $\phi^\dagger \psi$  at  $m_\phi = 0$  and  $M_\pi = 0.75 \text{ GeV}$ . The unit of vertical (horizontal) axis is  $a^{-1}$  (a). For large  $t$ , there is a plateau region and the correlator  $G(t)$  for the scalar-quark meson is fitted in the corresponding region by single exponential function. The vertical dashed lines denote the fit ranges of corresponding correlators.

effective masses, we can see the plateau regions. We note here that error estimate is done by the jackknife method for all the data in this study.

#### IV. RESULTS FOR SCALAR-QUARK HADRONS

In this section, we show lattice results for the mass of scalar-quark hadrons, namely, scalar-quark meson  $\phi^\dagger \phi$  and scalar-quark baryon  $\phi \phi \phi$ . Figure 4(a) shows scalar-quark meson mass  $M_{\phi^\dagger \phi}$  plotted against the bare scalar-quark mass  $m_\phi$ . The numerical data for this figure are listed in table IV. In Fig. 4(a), the large mass of scalar-quark meson about 3GeV is observed even for zero bare scalar-quark mass. This is very large compared to the ordinary mesons composed of light quarks. Figure 4(b)

FIG. 4: (a) Scalar-quark meson mass  $M_{\phi^\dagger \phi}$  and (b) scalar-quark baryon mass  $M_{\phi \phi \phi}$  plotted against the bare scalar-quark mass  $m_\phi$  in the unit of GeV. (c) Scalar-meson mass squared  $M_{\phi^\dagger \phi}^2$  and (d) scalar-quark baryon mass squared  $M_{\phi \phi \phi}^2$  plotted against  $m_\phi^2$  with  $m_\phi \geq 0$  and  $m_\phi^2 < 0$  in the unit of  $\text{GeV}^2$ . Calculations can be performed even with  $m_\phi \leq 0$ . Large mass of the meson about 3GeV and the baryon about 4.7 GeV at vanishing  $m_\phi$  can be seen.

shows scalar-quark baryon mass  $M_{\phi \phi \phi}$  plotted against  $m_\phi$ . In Fig. 4(b), large scalar-quark baryon mass about 4.7GeV is observed for zero bare scalar-quark mass. From the data of scalar-quark hadrons, constituent scalar-quark picture seems to be satisfied, i.e.,  $M_{\phi^\dagger \phi} \simeq 2M_\phi$  and  $M_{\phi \phi \phi} \simeq 3M_\phi$ , where  $M_\phi$  is the constituent (dynamically generated) scalar-quark mass and is 1.5-1.6GeV. Therefore, in the scalar-quark hadron systems, there occurs large mass generation of scalar-quarks (large quantum correction to bare scalar-quark mass) in strong interaction without chiral symmetry breaking.

In the quark system, we cannot obtain the propagator of quarks at  $m_\psi = 0$  on lattice. However, in the scalar-quark system, we can obtain the propagator of scalar-quarks even at  $m_\phi = 0$ . Figs. 4(c) and 4(d) shows the scalar-quark meson squared  $M_{\phi^\dagger \phi}^2$  and scalar-quark baryon mass squared  $M_{\phi \phi \phi}^2$  including the results

TABLE IV: The mass of scalar-quark hadrons: scalar-quark meson  $\phi^\dagger\phi$  and the scalar-quark baryon  $\phi\phi\phi$ , in term of the bare scalar-quark mass  $m_\phi$  at  $a^{-1} \simeq 1.1\text{GeV}$ .  $M_{\phi^\dagger\phi}$  and  $M_{\phi\phi\phi}$  denote their mass. The unit of mass is GeV.  $\chi^2$  over degrees of freedom  $N_{\text{df}}$  and fit ranges are also listed. Error estimate is done by the jackknife method.

| $m_\phi$ | $M_{\phi^\dagger\phi}$ ( $\chi^2/N_{\text{df}}$ , [fit range]) | $M_{\phi\phi\phi}$ ( $\chi^2/N_{\text{df}}$ , [fit range]) |
|----------|--|--|
| 0        | $3.016 \pm 0.0039$ (0.875, [7-14])                             | $4.697 \pm 0.0096$ (0.403, [7-15])                         |
| 0.11     | $3.025 \pm 0.0039$ (0.878, [7-14])                             | $4.711 \pm 0.0096$ (0.407, [7-15])                         |
| 0.22     | $3.052 \pm 0.0039$ (0.886, [7-14])                             | $4.751 \pm 0.0095$ (0.417, [7-15])                         |
| 0.33     | $3.095 \pm 0.0038$ (0.899, [7-14])                             | $4.818 \pm 0.0094$ (0.435, [7-15])                         |

for  $m_\phi^2 < 0$  plotted against  $m_\phi^2$ . Table V is the numerical data with  $m_\phi^2 < 0$ . Propagators of  $\phi$  can be calculated even with  $m_\phi^2 < 0$ , and the calculation breaks down at about  $m_\phi^2 = -(1.2\text{GeV})^2$ . This is due to the large quantum correction of  $m_\phi$ . In Fig. 4(c) and 4(d), we can see the linear dependence of  $M_{\phi^\dagger\phi}^2$  and  $M_{\phi\phi\phi}^2$  on  $m_\phi^2$ . More precisely, the relations  $M_{\phi^\dagger\phi}^2 = 4m_\phi^2 + \text{const.}$  and  $M_{\phi\phi\phi}^2 = 9m_\phi^2 + \text{const.}$  are approximately satisfied. The relations imply  $M_\phi^2 = m_\phi^2 + \Sigma_\phi$ , where  $\Sigma_\phi$  denotes the self-energy of scalar-quark  $\phi$ , if we assume  $M_{\phi^\dagger\phi} = 2M_\phi$  and  $M_{\phi\phi\phi} = 3M_\phi$ . This is the natural relation between renormalized mass and bare mass for scalar particles.

## V. RESULTS FOR CHIMERA HADRONS

Next, we show lattice QCD results for the mass of chimera hadrons: chimera meson  $\phi^\dagger\psi$ , chimera baryon  $\psi\psi\phi$  and  $\phi\phi\psi$ . Figures 5, 6 and 7 show the mass of chimera meson  $\phi^\dagger\psi$ , chimera baryon  $\psi\psi\phi$  and  $\phi\phi\psi$  plotted against corresponding pion mass  $M_\pi^2$ . The panels (a), (b), (c) and (d) of each figure are the masses of each hadron at  $m_\phi = 0, 110, 220$  and  $330\text{MeV}$ , respectively, plotted against  $M_\pi^2$ . The data at  $M_\pi^2 = 0$  is obtained from linear extrapolation and the solid lines denote the best-fit linear functions of the data. In panel (e) of each figure, the central values of panels (a) (b) (c) (d) are plotted all together. Different symbols of panel (e) of each figure correspond to the different bare scalar-quark mass  $m_\phi$  (circle:  $m_\phi=0$ , square:  $m_\phi=0.11\text{GeV}$ , triangle:  $m_\phi=0.22\text{GeV}$ , diamond:  $m_\phi=0.33\text{GeV}$ ). Table VI is the summary of the mass of chimera hadrons.

In Fig. 5, the large mass of chimera meson  $\phi^\dagger\psi$  can be seen. The extrapolated value of  $M_{\phi^\dagger\psi}$  at  $M_\pi^2 = 0$  and  $m_\phi = 0$  is  $1.86\text{GeV}$ . Similar to scalar-quark hadron masses,  $M_{\phi^\dagger\psi}$  is very large compared to ordinary low-lying mesons composed of light quarks. Also, constituent scalar-quark and quark picture is well satisfied, i.e.,  $M_{\phi^\dagger\psi} \simeq M_\phi + M_\psi$  for  $M_\phi \simeq 1.5\text{GeV}$  and  $M_\psi \simeq 400\text{MeV}$ . Constituent scalar-quark mass  $M_\phi \simeq 1.5\text{GeV}$  is consistent with that estimated from scalar-quark hadron masses. Concerning the dependence of  $m_\phi$  and  $M_\pi$ ,  $m_\phi$  dependence is rather weak compared to  $M_\pi$ . In fact, the mass difference between  $M_{\phi^\dagger\psi}(m_\phi = 0, M_\pi^2 = 0)$  and  $M_{\phi^\dagger\psi}(m_\phi = 0.33\text{GeV}, M_\pi^2 = 0)$  is only  $43\text{MeV}$ , although the difference of  $m_\phi$  is  $330\text{MeV}$  (we refer the mass  $M$  at  $m_\phi = \alpha$  and  $M_\pi = \beta$  to  $M(m_\phi = \alpha, M_\pi^2 = \beta^2)$ ). On

the other hand, the mass difference between  $M_{\phi^\dagger\psi}(m_\phi = 0, M_\pi^2 = 0)$  and  $M_{\phi^\dagger\psi}(m_\phi = 0, M_\pi^2 = (0.75\text{GeV})^2)$  is about  $120\text{MeV}$ . This value is the same order of the difference of  $m_\psi$ ,  $\delta m_\psi \simeq 190\text{MeV}$ , estimated from the relation  $2m_\psi a = 1/\kappa - 1/\kappa_c$ .

As for the chimera baryon  $\psi\psi\phi$ , the same tendency as that of chimera meson can be seen in Fig. 6. Constituent scalar-quark and quark picture is satisfied:  $M_{\psi\psi\phi} \simeq M_\phi + 2M_\psi$  for  $M_\phi \simeq 1.5\text{GeV}$  and  $M_\psi \simeq 400\text{MeV}$ .  $m_\phi$  dependence of  $M_{\psi\psi\phi}$  is weak and is almost the same as that of chimera meson. For  $M_\pi$  dependence, the difference between  $M_{\phi^\dagger\psi}(m_\phi = 0, M_\pi^2 = 0)$  and  $M_{\phi^\dagger\psi}(m_\phi = 0, M_\pi^2 = (0.75\text{GeV})^2)$  is about  $320\text{MeV}$ . This is about the same value of  $2\delta m_\psi \simeq 380\text{MeV}$ . The factor 2 is from the fact that chimera baryon  $\psi\psi\phi$  includes two  $\psi$ 's.

We can see that chimera baryon  $\phi\phi\psi$  has the same feature as chimera meson  $\phi^\dagger\psi$  and chimera baryon  $\psi\psi\phi$  in Fig. 7. Constituent scalar-quark and quark picture,  $M_{\phi\phi\psi} \simeq 2M_\phi + M_\psi$  for  $M_\phi \simeq 1.6\text{GeV}$  and  $M_\psi \simeq 400\text{MeV}$ , is satisfied. The magnitude of  $m_\phi$  dependence of  $M_{\phi\phi\psi}$  is about two times larger than that of chimera meson, because chimera baryon  $\phi\phi\psi$  has two  $\phi$ 's.  $m_\psi$  dependence is almost the same as that of chimera meson.

Here we note that the similarity of the structure between chimera meson  $\phi^\dagger\psi$  and chimera baryon  $\phi\phi\psi$ . We can see in Figs. 5 and 7 that  $M_\pi$  dependence of chimera meson  $\phi^\dagger\psi$  and chimera baryon  $\phi\phi\psi$  are almost the same within the errorbars. This is understood by the following non-relativistic picture. Due to the large mass of scalar-quark, wave function of  $\phi^\dagger$  in chimera meson  $\phi^\dagger\psi$  is localized and wavefunction of  $\psi$  distributes around the heavy anti scalar-quark. On the other hand, for chimera baryon  $\phi\phi\psi$ , two  $\phi$ 's get close in one-gluon exchange Coulomb potential due to their heavy masses. Therefore, two  $\phi$ 's behave like a point-like “di-scalar-quark”. As a result, the structure of chimera baryon  $\phi\phi\psi$  is similar to that of chimera meson  $\phi^\dagger\psi$ : the wavefunction of  $\phi\phi$  is localized and that of  $\psi$  distributes around  $\phi\phi$  (see Fig. 8). The difference between these two systems is only the mass of the heavy object ( $M_\phi$  for  $\phi^\dagger\psi$  and  $2M_\phi$  for  $\phi\phi\psi$ ). The heavy-light system is mainly characterized by the light object, because the heavy object only give the potential and the reduced mass in the system is almost the mass of light object. Such a similarity between chimera meson and chimera baryon is originated from the large quantum correction of bare scalar-quark mass  $m_\phi$ .

TABLE V: The mass of scalar-quark hadrons in the region  $m_\phi^2 < 0$ . Notations, units and error estimate are the same as those of table IV.

| $m_\phi^2$  | $M_{\phi^\dagger\phi}$ ( $\chi^2/N_{\text{df}}$ , [fit range]) | $M_{\phi\phi\phi}$ ( $\chi^2/N_{\text{df}}$ , [fit range]) |
|-------------|--|--|
| $-(0.11)^2$ | $3.007 \pm 0.0039$ (0.873, [7-14])                             | $4.684 \pm 0.0096$ (0.400, [7-15])                         |
| $-(0.22)^2$ | $2.979 \pm 0.0039$ (0.864, [7-14])                             | $4.642 \pm 0.0097$ (0.390, [7-15])                         |
| $-(0.33)^2$ | $2.932 \pm 0.0040$ (0.847, [7-14])                             | $4.571 \pm 0.0098$ (0.372, [7-15])                         |

TABLE VI: The mass of chimera hadrons (bound states of scalar-quarks  $\phi$  and quarks  $\psi$ ) in term of the bare scalar-quark mass  $m_\phi$  and hopping parameter  $\kappa$  at  $a^{-1} \simeq 1.1\text{GeV}$ .  $M_{\phi^\dagger\psi}$ ,  $M_{\psi\psi\phi}$  and  $M_{\phi\phi\psi}$  denote the mass of chimera mesons  $\phi^\dagger\psi$  and chimera baryons ( $\psi\psi\phi$ ,  $\phi\phi\psi$ ), respectively. The unit is GeV.  $\chi^2/N_{\text{df}}$  and fit ranges are also listed. The values at  $\kappa = \kappa_c$  are obtained from linear extrapolation. Error estimate is done by the jackknife method.

| $m_\phi$ | $\kappa$   | $M_{\phi^\dagger\psi}$ ( $\chi^2/N_{\text{df}}$ , [fit range]) | $M_{\psi\psi\phi}$ ( $\chi^2/N_{\text{df}}$ , [fit range]) | $M_{\phi\phi\psi}$ ( $\chi^2/N_{\text{df}}$ , [fit range]) |
|----------|------------|--|--|--|
| 0.00     | $\kappa_c$ | $1.862 \pm 0.013$  | $2.230 \pm 0.037$  | $3.558 \pm 0.029$  |
|          | 0.1650     | $1.914 \pm 0.008$ (0.485, [7-12])                              | $2.366 \pm 0.022$ (0.041, [8-11])                          | $3.607 \pm 0.017$ (0.142, [7-12])                          |
|          | 0.1625     | $1.950 \pm 0.007$ (0.437, [7-12])                              | $2.464 \pm 0.018$ (0.173, [8-11])                          | $3.637 \pm 0.014$ (0.220, [7-12])                          |
|          | 0.1600     | $1.986 \pm 0.006$ (0.460, [7-12])                              | $2.558 \pm 0.016$ (0.615, [8-11])                          | $3.672 \pm 0.013$ (0.383, [7-12])                          |
|          | 0.11       | $1.867 \pm 0.013$  | $2.235 \pm 0.037$  | $3.568 \pm 0.029$  |
|          | 0.1650     | $1.929 \pm 0.008$ (0.483, [7-12])                              | $2.371 \pm 0.022$ (0.043, [8-11])                          | $3.616 \pm 0.017$ (0.143, [7-12])                          |
|          | 0.1625     | $1.955 \pm 0.007$ (0.436, [7-12])                              | $2.470 \pm 0.018$ (0.169, [8-11])                          | $3.646 \pm 0.014$ (0.220, [7-12])                          |
|          | 0.1600     | $1.991 \pm 0.006$ (0.459, [7-12])                              | $2.564 \pm 0.016$ (0.608, [8-11])                          | $3.681 \pm 0.013$ (0.383, [7-12])                          |
|          | 0.22       | $1.883 \pm 0.013$  | $2.250 \pm 0.037$  | $3.596 \pm 0.029$  |
|          | 0.1650     | $1.934 \pm 0.008$ (0.478, [7-12])                              | $2.386 \pm 0.022$ (0.051, [8-11])                          | $3.644 \pm 0.017$ (0.145, [7-12])                          |
|          | 0.1625     | $1.969 \pm 0.007$ (0.432, [7-12])                              | $2.484 \pm 0.018$ (0.155, [8-11])                          | $3.674 \pm 0.014$ (0.219, [7-12])                          |
|          | 0.1600     | $2.005 \pm 0.006$ (0.454, [7-12])                              | $2.578 \pm 0.016$ (0.587, [8-11])                          | $3.709 \pm 0.013$ (0.382, [7-12])                          |
|          | 0.33       | $1.905 \pm 0.013$  | $2.273 \pm 0.038$  | $3.643 \pm 0.029$  |
|          | 0.1650     | $1.957 \pm 0.008$ (0.470, [7-12])                              | $2.409 \pm 0.023$ (0.064, [8-11])                          | $3.690 \pm 0.017$ (0.150, [7-12])                          |
|          | 0.1625     | $1.993 \pm 0.007$ (0.425, [7-12])                              | $2.507 \pm 0.018$ (0.135, [8-11])                          | $3.720 \pm 0.014$ (0.216, [7-12])                          |
|          | 0.1600     | $2.029 \pm 0.006$ (0.454, [7-12])                              | $2.601 \pm 0.016$ (0.554, [8-11])                          | $3.754 \pm 0.013$ (0.381, [7-12])                          |

## VI. CONCLUSION AND DISCUSSION

We have studied the light scalar-quarks  $\phi$  and their color-singlet hadronic states with quenched  $SU(3)_c$  lattice QCD in terms of their mass generation. We have investigated the scalar-quark bound states (scalar-quark hadrons): scalar-quark meson  $\phi^\dagger\phi$  and scalar-quark baryon  $\phi\phi\phi$ . We have also investigated the bound states of scalar-quarks and quarks, which we name “chimera hadrons”: chimera meson  $\phi^\dagger\psi$ , chimera baryons  $\psi\psi\phi$  and  $\phi\phi\psi$ . For the lattice QCD calculation, we have adopted the standard Wilson action for gluon sector and the Wilson fermion action for quark sector. The lattice action of scalar-quark is local and the simplest one which is gauge invariant. We have adopted  $\beta \equiv 2N_c/g^2 = 5.70$ , which corresponds to the lattice spacing  $a \simeq 0.18\text{fm} = (1.1\text{GeV})^{-1}$ , and lattice size  $16^3 \times 32$  (spatial volume  $V = (2.9\text{fm})^3$ ). We have used 100 gauge configurations in the interval of 500 sweeps after 20000 thermalization. For the bare scalar-quark mass, we have adopted  $m_\phi = 0.0, 0.11, 0.22$  and  $0.33\text{GeV}$ , and for the bare quark mass,  $\kappa = 0.1650, 0.1625$  and  $0.1600$ . Fitting the temporal correlator of each new-type hadrons by single exponential function, we have extracted the mass of lowest state of the hadrons.

For the scalar-quark hadrons, we have found their large mass. The masses of scalar-quark meson  $\phi^\dagger\phi$  and scalar-quark baryon  $\phi\phi\phi$  at the vanishing  $m_\phi$  and  $M_\pi$

are about  $3\text{GeV}$  and  $4.7\text{GeV}$ , respectively. Constituent scalar-quark picture is almost satisfied, i.e.,  $M_{\phi^\dagger\phi} \simeq 2M_\phi$  and  $M_{\phi\phi\phi} \simeq 3M_\phi$ , where  $M_\phi$  is the constituent scalar-quark mass about  $1.5\text{GeV}$ . We have also found that even in the case of  $m_\phi^2 < 0$ , the calculation can be performed until about  $m_\phi^2 = -(1.2\text{GeV})^2$ .  $m_\phi$  dependence of scalar-quark hadron masses squared is linear with respect to  $m_\phi^2$ . This is natural because the relation between the constituent scalar-quark mass  $M_\phi$  and bare scalar-quark mass  $m_\phi$  is written as  $M_\phi^2 = m_\phi^2 + \Sigma_\phi$ . For the chimera hadrons, we have also found their large masses:  $M_{\phi^\dagger\psi} \simeq 1.9\text{GeV}$ ,  $M_{\psi\psi\phi} \simeq 2.2\text{GeV}$  and  $M_{\phi\phi\psi} \simeq 3.6\text{GeV}$ , for vanishing  $m_\phi$  and  $M_\pi$ . The constituent scalar-quark and quark picture is also satisfied, i.e.,  $M_{m\phi+n\psi} \simeq mM_\phi + nM_\psi$ , where constituent scalar-quark mass  $M_\phi = 1.5\text{--}1.6\text{GeV}$  and constituent quark mass  $M_\psi = 400\text{MeV}$ .  $m_\phi$  dependence of chimera-hadron masses is weak and the bare quark mass  $m_\psi$  seems to govern their systems in our calculated range of  $m_\phi$  and  $m_\psi$ . Due to the large mass generation of  $\phi$ , there occurs similarity of the structure between chimera meson  $\phi^\dagger\psi$  and chimera baryon  $\phi\phi\psi$ .

The large mass generation of the scalar-quark  $\phi$  reflects the general argument of large quantum corrections for scalar particles. As other famous example, the Higgs scalar field suffers from large radiative corrections in the Grand Unified Theory (GUT), and to realize the low-lying mass of the Higgs scalar inevitably requires “fine tuning” related to the gauge hierarchy prob-

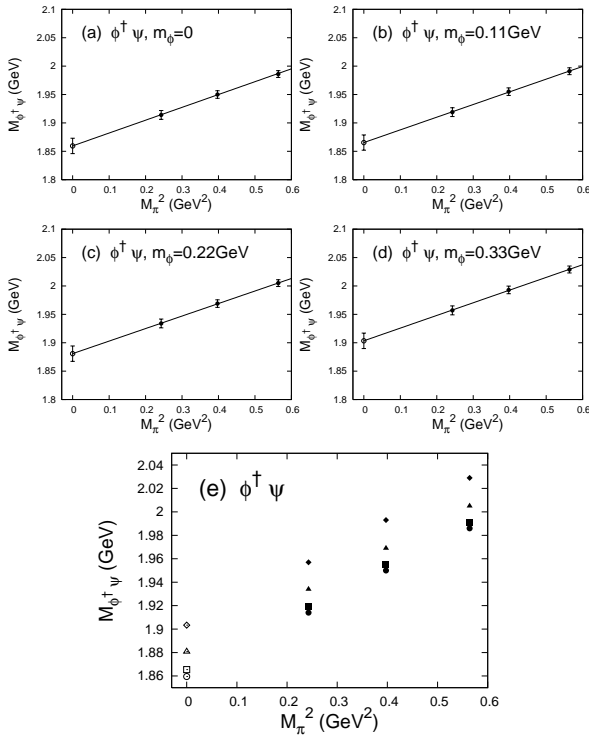


FIG. 5: Mass of chimera meson,  $M_{\phi^\dagger \psi}$ , plotted against pion mass squared  $M_\pi^2$  in the unit of  $\text{GeV}^2$ . Fig. 5(a), 5(b), 5(c) and 5(d) are  $M_{\phi^\dagger \psi}$  at  $m_\phi = 0, 110, 220$  and  $330 \text{ MeV}$ , respectively, plotted against  $M_\pi^2$ . The data at  $M_\pi^2 = 0$  is obtained from linear extrapolation, and the solid line denote the best-fit linear function of the data. In Fig. 5(e), the central values of Figs. 5(a), 5(b), 5(c) and 5(d) are plotted all together. Different symbols of Fig. 5(e) correspond to the different bare scalar-quark mass  $m_\phi$  (circle:  $m_\phi=0$ , square:  $m_\phi=0.11 \text{ GeV}$ , triangle:  $m_\phi=0.22 \text{ GeV}$ , diamond:  $m_\phi=0.33 \text{ GeV}$ ).

lem [21, 26]. In fact, while the typical energy scale of the electro-weak unification is about  $O(10^2 \text{ GeV})$  and the Higgs scalar mass is to be also  $O(10^2 \text{ GeV})$ , the GUT scale, i.e., the typical energy scale of the electro-weak and strong unification, is conjectured to be extremely large as  $E_{\text{GUT}} \sim 10^{15-16} \text{ GeV}$ . In the simple GUT scenario, the standard model is regarded as an effective theory applicable up to the GUT scale  $E_{\text{GUT}}$ , which can be identified as the cutoff scale of the standard model as  $\Lambda \sim E_{\text{GUT}}$ . For the self-energy of the Higgs scalar,  $\Sigma_H$ , there appears a large quantum correction including second-order divergence as  $\Sigma_H \propto \Lambda^2$ , with the cutoff parameter  $\Lambda$ . This is because scalar particles do not have symmetry restriction like the chiral symmetry for light fermions and the gauge symmetry for vector gauge bosons. Therefore, it is natural that the Higgs scalar receives huge quantum correction of order  $E_{\text{GUT}}$ , and, in order to realize the low-lying physical Higgs mass of order  $10^2 \text{ GeV}$ , an extreme fine tuning is necessary for the bare mass of the Higgs scalar. This is the problem of fine tuning for the Higgs scalar. In lattice QCD, the self-energy of scalar-quarks  $\Sigma_\phi$  also

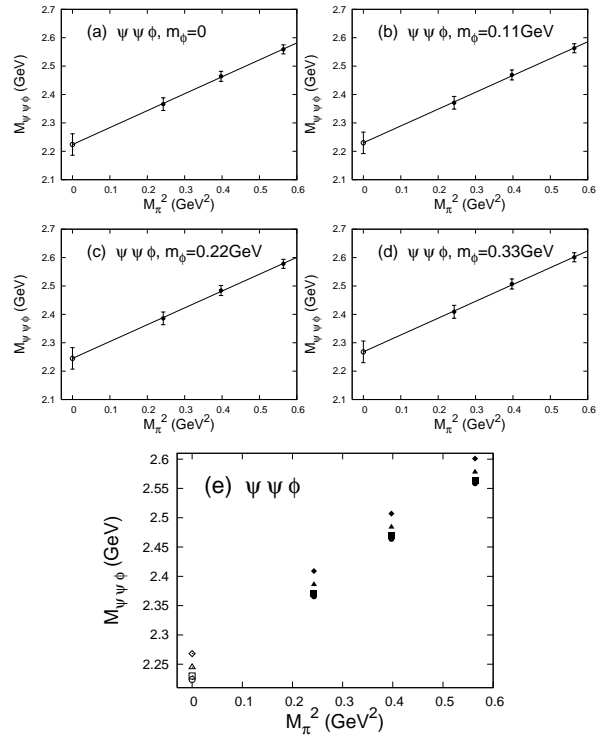


FIG. 6: Mass of chimera baryon,  $M_{\psi \psi \phi}$ , plotted against pion mass squared  $M_\pi^2$  in the unit of  $\text{GeV}^2$ . The notation, unit and notices are same as that of Fig. 5.

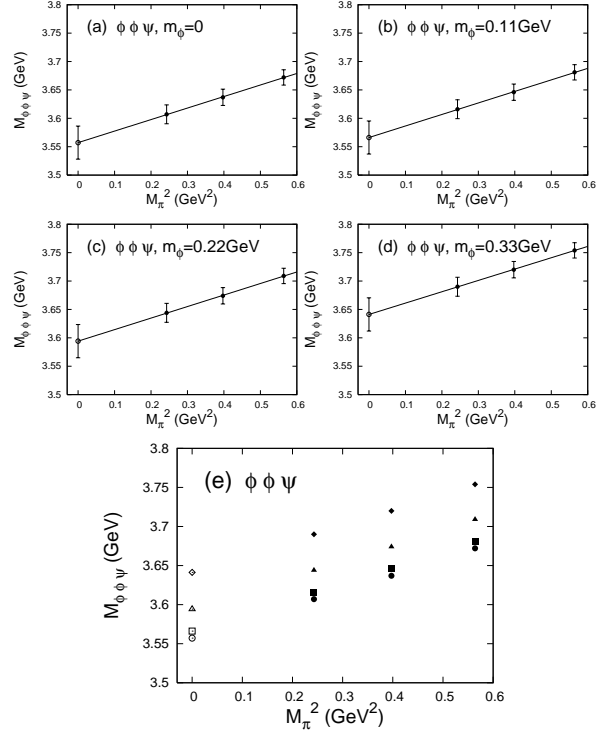


FIG. 7: Mass of chimera baryon,  $M_{\phi \phi \psi}$ , plotted against pion mass squared  $M_\pi^2$  in the unit of  $\text{GeV}^2$ . The notation, unit and notices are same as that of Fig. 5.

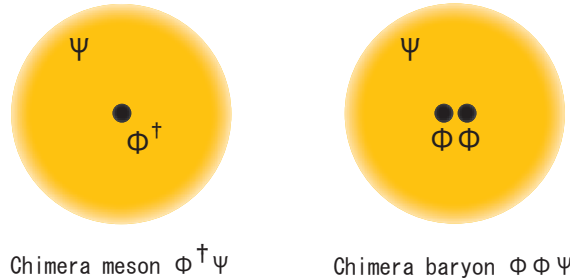


FIG. 8: Structure of chimera meson  $\phi^\dagger\psi$  and chimera baryon  $\phi\phi\psi$ . Wavefunction of quark  $\psi$  in chimera meson distributes around the heavy scalar-quark  $\phi^\dagger$ . Similar to chimera meson, wavefunction of  $\psi$  in chimera baryon distributes around the localized wavefunction of two  $\phi$ 's.



FIG. 9: Schematic figure for dynamical mass generation of colored particles. Even without chiral symmetry breaking, colored particles generally acquire a large effective mass due to dressed gluons.

receives a large quantum correction including the second-order divergence as  $\Sigma_\phi \sim \Lambda^2$ , similar to the Higgs scalar. Since the constituent mass  $M_\phi$  of the scalar-quark satisfies the relation of  $M_\phi^2 = m_\phi^2 + \Sigma_\phi$  with the bare mass  $m_\phi$  from a general argument of the scalar field, even at  $m_\phi = 0$ , the constituent scalar-quark mass  $M_\phi$  takes a large value as  $M_\phi = \Sigma^{1/2} \sim \Lambda$ . Note here that the lattice QCD can be regarded as a cutoff theory with the cutoff about the lattice spacing as  $\Lambda \sim a^{-1}$ . Actually, the quantum correction to the scalar-quark mass is found to

be about 1.5GeV in this lattice study, which is approximately the same order of the cutoff scale  $a^{-1} \simeq 1.1\text{GeV}$ . In this way, the large quantum correction to the scalar-quarks is explained naturally.

In terms of the diquark picture, we find that the point-like diquarks interacting with gauge fields have large mass about 1.5GeV at the cutoff  $a^{-1} \sim 1\text{GeV}$  which is about the hadronic scale. The diquark mass of about 1.5 GeV is too heavy to use in effective models of hadrons. Therefore, the lattice result indicates that the simple modeling which treats the diquark as a local scalar field at the scale of  $a^{-1} \sim 1\text{GeV}$  in QCD is rather dangerous. If we treat the diquark as a point-like object, we must do the subtle tuning of the diquark model, and the model cannot be so simple one like QCD.

In this way, even without chiral symmetry breaking, large dynamical mass generation occurs for the scalar-quark systems as scalar-quark/chimera hadrons. Together with the large glueball mass ( $> 1.5\text{GeV}$ ) and large difference ( $\sim 400\text{MeV}$ ) between current and constituent charm-quark masses, this type of mass generation would be generally occurred in the strong interaction, and therefore we conjecture that all colored particles generally acquire a large effective mass due to dressed gluon effects as shown in Fig. 9.

### Acknowledgments

H. S. is supported in part by the Grant for Scientific Research [(C) No. 16540236] from the Ministry of Education, Culture, Sports, Science and Technology, Japan. H. I. and T.T. T. are supported by the Japan Society for the Promotion of Science for Young Scientists. Our lattice QCD calculations have been performed on NEC-SX5 and NEC-SX8 at Osaka University.

---

[1] P. W. Higgs, Phys. Lett. **12**, 132, 1964.  
[2] Particle Data Group (W.M. Yao et al.), J. Phys. G**33**, 1 (2006).  
[3] A. De Rujula, H. Georgi, and S. L. Glashow, Phys. Rev. D**12**, 147(1975).  
[4] Y. Nambu and G. Jona-Lasinio, Phys. Rev. **122**, 345 (1961); Phys. Rev. **124**, 246 (1961).  
[5] J.B. Kogut, M. Stone, H.W. Wyld, W.R. Gibbs, J. Shigemitsu, S.H. Shenker, and D.K. Sinclair, Phys. Rev. Lett. **50**, 393 (1983).  
[6] T. Hatsuda and T. Kunihiro, Phys. Rept. **247**, 221-367 (1994).  
[7] H. Iida, M. Oka, and H. Suganuma, Eur. Phys. J. A**23**, 305 (2005); Nucl. Phys. B**141** (Proc. Suppl), 191 (2005).  
[8] C. DeTar and J.B. Kogut, Phys. Rev. Lett. **59**, 399 (1987); Phys. Rev. D**36**, 2828 (1987).  
[9] T. Hatsuda and S.H. Lee, Phys. Rev. C**46**, R34 (1992).  
[10] CERES Collaboration (G. Agakichiev et al.), Phys. Rev. Lett. **75**, 1272 (1995).  
[11] R. Muto et al., Nucl. Phys. A**774**, 723-726 (2006).  
[12] J.E. Mandula and M. Ogilvie, Phys. Lett. B**185**, 127 (1987).  
[13] K. Amemiya and H. Suganuma, Phys. Rev. D**60**, 114509 (1999).  
[14] C.J. Morningstar and M. Peardon, Phys. Rev. D**60**, 034509 (1999); N. Ishii, H. Suganuma, and H. Matsufuru, Phys. Rev. D**66**, 094506 (2002).  
[15] F.E. Close and R.G. Roberts, Z. Phys. C**8**, 57 (1981).  
[16] S. Fredriksson, M. Jandel, and T. Larsson, Z. Phys. C**14**, 35 (1982).  
[17] M.I. Pavkovic, Phys. Rev. D**14**, 3186 (1976).  
[18] F. Wilczek, “Diquarks as Inspiration and as Objects”, hep-ph/0409168.  
[19] D. Bailin and A. Love, Phys. Rept. **107**, 325-385 (1984).  
[20] M. Alford, K. Rajagopal, and F. Wilczek, Nucl. Phys. B**537**, 443 (1999).  
[21] T.P. Cheng and L.F. Li, “Gauge theory of elementary particle physics”, Oxford University Press (1988).

- [22] H. Iida, H. Suganuma, and T.T. Takahashi, hep-lat/0612019, to be published in AIP Conf. Proc..
- [23] H.J. Rothe, “Lattice gauge theories (3rd edition)”, World Scientific (2005), and references therein.
- [24] T.T. Takahashi, H. Matsufuru, Y. Nemoto, and H. Suganuma, Phys. Rev. Lett. **86**, 18 (2001); T.T. Takahashi, H. Suganuma, Y. Nemoto, and H. Matsufuru, Phys. Rev. D**65**, 114509 (2002).
- [25] F. Butler, H. Chen, J. Sexton, A. Vaccarino, and D. Weingarten, Nucl. Phys. **B430**, 179-228 (1994); T.T. Takahashi, T. Umeda, T. Onogi, and T. Kunihiro, Phys. Rev. D**71**, 114509 (2005).
- [26] M.E. Peskin and D.V. Schroeder, “An Introduction to Quantum Field Theory”, Perseus Books Publishing (1995).